Magnetic and electrical properties of p-type Mn-doped $CuCrO_2$ semiconductors

2009 J. Phys. D: Appl. Phys. 42 055009

(http://iopscience.iop.org/0022-3727/42/5/055009)

IOP PUBLISHING JOURNAL OF PHYSICS D: APPLIED PHYSICS

J. Phys. D: Appl. Phys. **42** (2009) 055009 (6pp) doi:10.1088/0022-3727/42/5/055009

Magnetic and electrical properties of p-type Mn-doped $CuCrO_2$ semiconductors

Da Li[1], Xiaodong Fang[1,3], Weiwei Dong[1], Zanhong Deng[1], Ruhua Tao[1], Shu Zhou[1], Jinmei Wang[1], Tao Wang[1], Yiping Zhao[1] and Xuebin Zhu[2]

[1] Key Lab of New Thin Film Solar Cells, Anhui Institute of Optics and Fine Mechanics, Chinese Academy of Sciences, Hefei 230031, People's Republic of China

[2] Key Laboratory of Materials Physics, Institute of Solid State Physics, Chinese Academy of Sciences, Hefei 230031, People's Republic of China

E-mail: lida@ustc.edu

Received 5 December 2008
Published 19 February 2009
Online at stacks.iop.org/JPhysD/42/055009

Abstract

Mn-doped $CuCrO_2$ polycrystalline semiconductors were synthesized by the sol–gel method. The valence state of the Mn ions in the $CuCr_{1-x}Mn_xO_2$ samples was identified as 3+ by analysing their lattice parameters, their electrical properties and their x-ray photoelectron spectra. The temperature dependence of the susceptibility of all samples exhibits paramagnetic behaviour at high temperature. For $x = 0.20$ the samples exhibit a clear ferromagnetic (FM) transition at 120 K. Clear hysteresis loops indicate that FM order exists in the Mn-doped samples at 50 K. All samples behave like semiconductors. The electrical and magnetic properties indicate that the ferromagnetism can be attributed to the double exchange interaction between the Mn^{3+} and Cr^{3+} in $CuCr_{1-x}Mn_xO_2$ semiconductors.

1. Introduction

Diluted magnetic semiconductors (DMSs) involve charge and spin degrees of freedom in a single substance and therefore have attracted much interest owing to their unique magnetic, magneto-optical and magneto-electrical effects. Possible spintronic devices are spin-valve transistors, spin light-emitting diodes and nonvolatile logic devices. Many investigations were devoted to integrating magnetic and semiconducting phenomena for the applications, as well as the fundamental understanding of the phenomena [1]. The synthesis of Mn-doped III–V-based ferromagnetic (FM) semiconductors such as InMnAs [2] and GaMnAs [3] has made it possible to fabricate spintronic devices. The theoretical prediction of the possibility of room-temperature ferromagnetism in p-type ZnO-based and GaN-based DMSs has stimulated research interest in this field again [4]. And ZnO [5, 6] is especially exciting because oxide semiconductors can be potentially used to inject spin-polarized carriers [7]. Generally, oxide semiconductors have wide band gaps, i.e. transparent for visible light. This feature serves an important role as transparent conducting oxides (TCOs) that are used for various applications such as transparent electrodes in flat panel displays and window layers in solar cells. Up to now, most of the oxide semiconductors (such as ZnO, $In_{1-x}Sn_xO_2$) extensively studied are n-type [8, 9]; there are few p-TCOs.

In 1997, Kawazoe *et al* reported that the delafossite structure $CuAlO_2$ was a p-type transparent semiconductor [10]. Among the delafossite structure oxides, the $CuCrO_2$ film has a conductivity of the order 1 scm^{-1}, and upon doping with 5% Mg the conductivity can be improved to 220 scm^{-1} which is the largest conductivity in p-TCOs [11]. In 2005, delafossite-based $CuAl_{1-x}Mn_xO_2$ bulks were studied, whereas there was no evidence for a FM transition above 2 K [12]. In the same year Kizaki *et al* predicted that a high-spin FM state was expected to be stable in p-type delafossite-based $Cu_{1-x}TM_xAlO_2$ (TM=Mn, Fe, Co, Ni) [13]. In this reaserch we successfully prepared Mn-doped $CuCrO_2$ semiconductors which exhibit FM transitions at about 120 K. The magnetic and electrical properties can be well explained by double exchange (DE) intereaction between Mn^{3+} and Cr^{3+}.

[3] Author to whom any correspondence should be addressed.

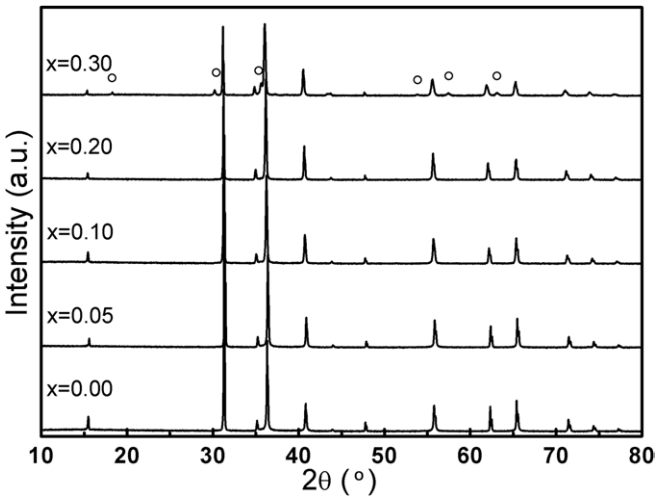

Figure 1. XRD patterns of $CuCr_{1-x}Mn_xO_2$ samples with a rhombohedral delafossite structure, Peaks labelled ◦ are diffraction peaks of impurities.

2. Experiments

Mn-doped $CuCrO_2$ polycrystalline semiconductors were prepared by the sol–gel method, which can shorten the annealing time and lower the annealing temperature compared with the conventional solid state reaction. Stoichiometric $Mn(CH_3COO)_2{\cdot}4H_2O$(99%)(99%), $Cu(CH_3COO)_2{\cdot}H_2O$ (99%) and $Cr(NO_3)_3{\cdot}9H_2O$(99%) were dissolved in distilled water with appropriate citric acid. The solution was then dried and pre-sintered to prepare powders. Finally, pressed pellets were sintered at 1373 K for 10 h in air [14], and Mn-doped $CuCrO_2$ semiconductors were obtained. The structure of the samples was confirmed by x-ray diffraction (XRD) using Cu K_α radiation ($\lambda = 1.5418$ Å). X-ray photoelectron spectroscopy (XPS) analysis was performed to ascertain the valence state of all elements in the $CuCr_{0.90}Mn_{0.10}O_2$ sample on an ESCALAB MK II system using an Al K_α source. The dc resistivity of all samples was measured with a four-probe configuration. The magnetic properties of these samples were investigated using the Physics Property Measurement System (PPMS).

3. Results and discussions

3.1. Structural properties

Figure 1 shows the XRD patterns for the $CuCr_{1-x}Mn_xO_2$ (x is nominal concentration) semiconductors prepared by the sol–gel method. It can be observed that the samples are single 3R delafossite structure for $x < 0.30$. The corresponding JCPDF Card No. of $CuCrO_2$ is 89-6744. There are some tiny diffraction peaks of impurities for $x = 0.30$. These impurities are likely to be cubic phase $CuCrMnO_4$, $CuCr_2O_4$ or $CuMn_2O_4$. They cannot be distinguished by XRD results because these impurities have the same crystal structure and similar lattice parameters. The lattice parameters a and c of the $CuCr_{1-x}Mn_xO_2$ ($0 \leqslant x \leqslant 0.30$) samples with their corresponding errors are shown in figure 2. With the increase

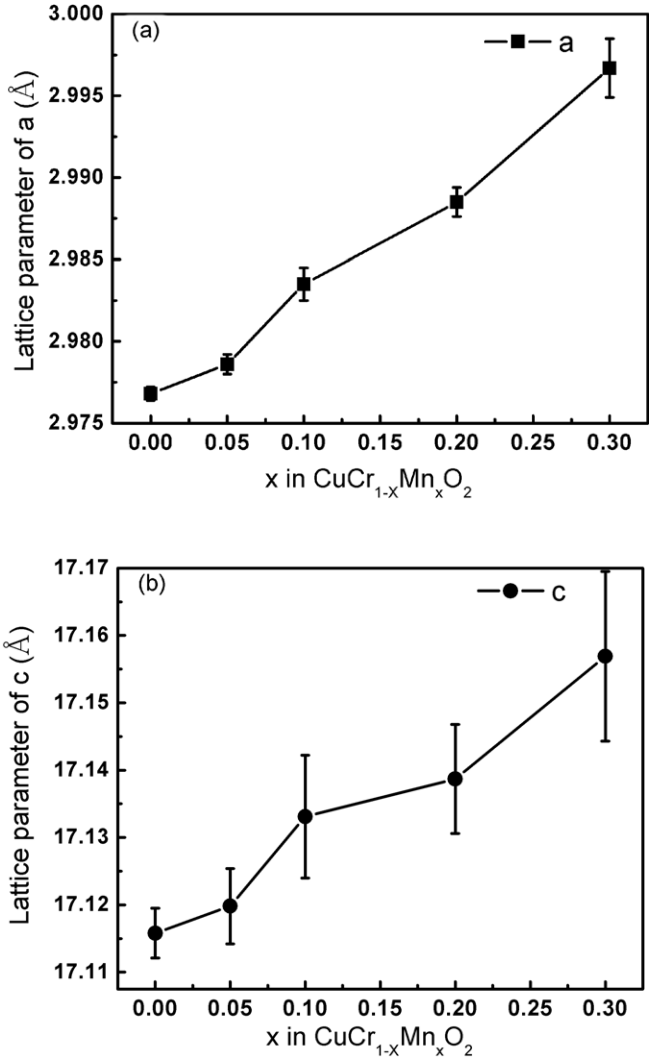

Figure 2. (*a*) Relationship between the lattice parameter a and the Mn concentration x of $CuCr_{1-x}Mn_xO_2$ samples; (*b*) relationship between the lattice parameter c and the Mn concentration x of $CuCr_{1-x}Mn_xO_2$ samples.

in the Mn concentration, the lattice parameters a and c increase almost linearly. It can be concluded that the valence of Mn ions was not 4+ according to the data of the ionic radius of Mn and Cr (Mn^{2+}: 0.80 Å, Mn^{3+}: 0.66 Å, Mn^{4+}: 0.60 Å and Cr^{3+}: 0.63 Å) as well as lattice expansion. The lattice parameters a and c would decrease if the valence state of the Mn ions is 4+ in Mn-doped $CuCrO_2$ semiconductors because the ionic radii of Mn^{4+} are smaller than that of Cr^{3+}. It can be confirmed that the valence state of Mn ions is 2+ or 3+. Moreover the changes in the lattice parameters a and c due to the increase in the Mn concentration are very small. Therefore, the valence state of the Mn ions presented in the samples should be 3+ since the ionic radius of Mn^{3+} is slightly larger than that of Cr^{3+}, whereas the valence state of Mn ions cannot be totally confirmed by the changes in the lattice parameters. Thereby XPS analysis of $CuCr_{0.90}Mn_{0.10}O_2$ was carried out in order to ascertain the valence state of all elements in $CuCr_{1-x}Mn_xO_2$ semiconductors.

Figure 3(*a*) shows the typical Cu 2p XPS spectra of the $CuCr_{0.90}Mn_{0.10}O_2$ semiconductor. The line shape of the Cu

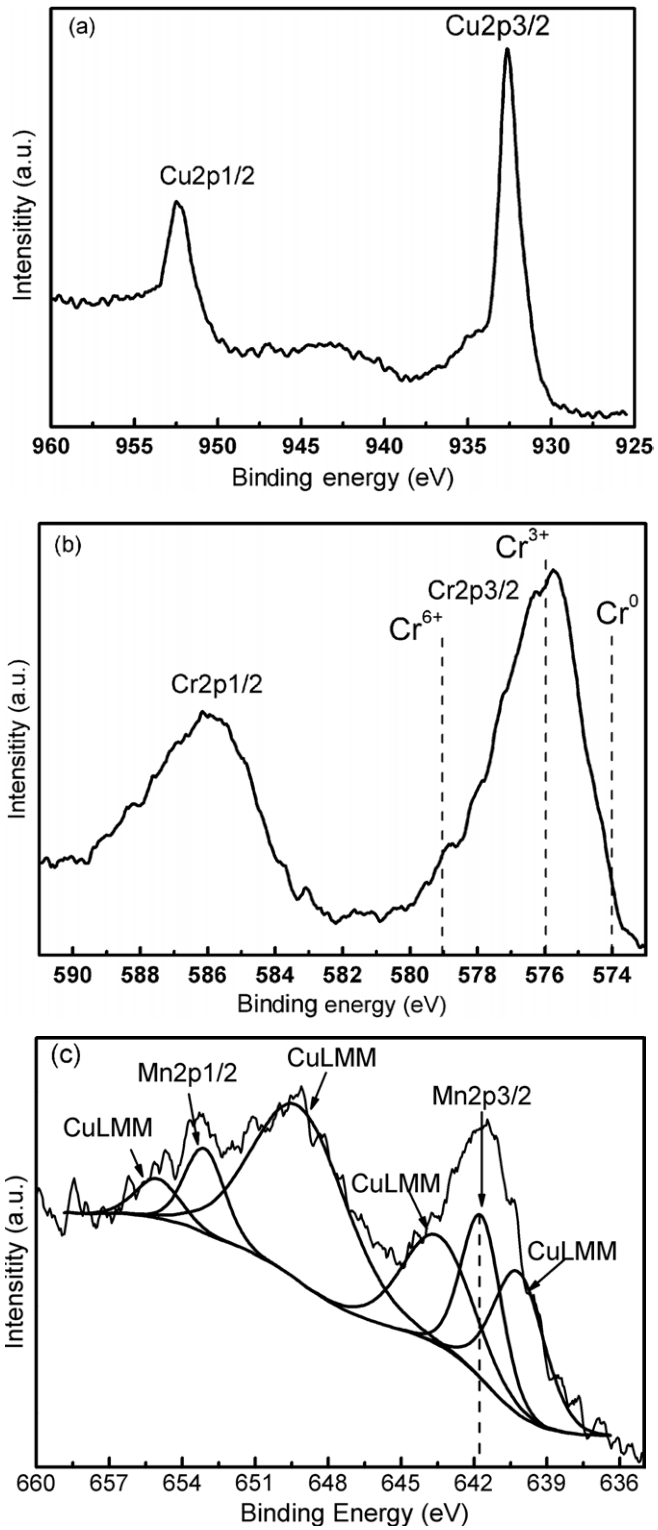

Figure 3. XPS spectra of the $CuCr_{0.90}Mn_{0.10}O_2$ semiconductor: (*a*) Cu 2p XPS spectra, (*b*) Cr 2p XPS spectra, (c) computer fitting curve of the Mn 2p XPS spectrum.

2p XPS spectra with no clear satellite is quite similar to that of $Cu_2O(Cu^{1+})$. It is thus concluded that the Cu ions in the $CuCr_{0.90}Mn_{0.10}O_2$ semiconductor are in the monovalent state [15]. The Cr 2p3/2 peak at 575.8 eV shown in figure 3(*b*) indicates that the valence state of Cr ions is 3+ [16]. Figure 3(*c*) shows the curve fitting results of the Mn 2p XPS spectra of the sample. The valence of the Mn ions is hard to determine because the binding energies for different valences of Mn ions are very close. And the position of the Mn 2p3/2 peak was difficult to confirm due to the influence of the Auger peaks of Cu. The centre of the Mn 2p3/2 peak was located at a binding energy of 641.7 eV. This result implies that the valence state of Mn ions is likely to be 3+ in the $CuCr_{0.90}Mn_{0.10}O_2$ semiconductor [17]. The electrical property of the $CuCr_{1-x}Mn_xO_2$ ($0 \leqslant x \leqslant 0.20$) samples was studied in order to confirm the valence state of Mn ions because the changes in electrical property would be different due to different valence states of Mn ions. If Mn^{2+} ions substituted for Cr^{3+} ions in the $CuCr_{1-x}Mn_xO_2$ semiconductors the hole concentration would increase, which would enhance the p-type conductivity of the samples. Otherwise, holes or electrons will not be produced if the valence state of Mn ions is 3+ in $CuCr_{1-x}Mn_xO_2$ semiconductors, whereas the doping Mn would enhance the distortion of the lattice, which would lead to an increase in the scattering of carriers [18]. Therefore, the increase in the Mn concentration would lead to a decrease in the carrier mobility. The resistivities would increase if Mn^{3+} ions substituted for Cr^{3+} ions. The thermopower (Seebeck coefficient) and dc resistivities of the samples were measured to observe the type of carrier and variation of resistivities (ρ) of the $CuCr_{1-x}Mn_xO_2$ ($0 \leqslant x \leqslant 0.20$) semiconductors.

3.2. Electrical properties

The type of carrier can be confirmed by the thermopower of the samples. The thermopower can be calculated by the following formula [19]:

$$Q = -\lim_{\Delta T \to 0} \frac{\Delta V}{\Delta T}. \tag{1}$$

We measured the thermopower of all the samples by making a temperature difference in the samples. The thermopower of all the samples was positive in nature at room temperature, which confirmed that the carrier is a hole in $CuCr_{1-x}Mn_xO_2$ ($0 \leqslant x \leqslant 0.20$) semiconductors. The temperature dependence of the resistivity of samples for $x < 0.30$ is shown in figure 4. The values of ρ at 300 K for $x = 0, 0.05, 0.10$ and 0.20 are $3.4 \times 10^3\ \Omega$ cm, $415 \times 10^3\ \Omega$ cm, $245 \times 10^3\ \Omega$ cm and $45 \times 10^3\ \Omega$ cm, respectively. The resistivity of the Mn doped samples is larger than that of a pure $CuCrO_2$ semiconductor. And the resistivity of the samples increases as the Mn concentration increases for $x \leqslant 0.10$. Therefore, we can conclude that the valence state of Mn ions is 3+ in the $CuCr_{1-x}Mn_xO_2$ samples. Otherwise for $x > 0.10$ the resistivity decreases as the Mn concentration increases. Maybe some interactions, which enhanced the hole mobility, exist in the $CuCr_{1-x}Mn_xO_2$ semiconductors. A DE-like interaction could occur through Mn^{3+}–O–Cr^{3+} in terms of an identical electronic configuration ($t_{2g}^3 e_g^0$) between Mn^{4+} and Cr^{3+} [20]. The DE mechanism was originally proposed by Zener for (La, A)MnO_3 (A = Ca, Sr or Ba) [21]. It is the replacement of A^{2+} for La^{3+} that results in the appearance of Mn^{4+} ions in these samples. As a result, an electron can jump from the Mn^{3+} site to the Mn^{4+} site leading to exchange coupling between the Mn^{3+} and Mn^{4+} ions. DE coupling between the Mn^{3+} and the Mn^{4+} ions is

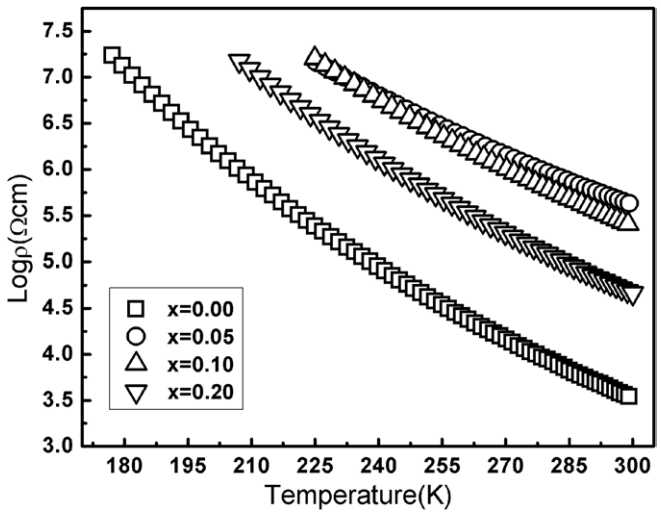

Figure 4. Temperature dependence of the resistivity of $CuCr_{1-x}Mn_xO_2$ semiconductors.

believed to be responsible for conductivity and ferromagnetism in the (La, A)MnO_3 system. The increase in the hole mobility could be due to this DE interaction between the Mn^{3+} and the Cr^{3+} ions. Thereby for $x \geqslant 0.10$ the resistivity of the samples decreased with the increase in Mn concentration. Otherwise, the DE interaction between the Mn^{3+} and the Cr^{3+} ions would be very weak because the resistivity of the doped samples is larger than the resistivity of the pure $CuCrO_2$ semiconductor. Mn^{3+}–O–Cr^{3+} exchange interaction was widely studied in the $LaMn_{1-x}Cr_xO_3$ system [22–25]. Ferromagnetism should exist in the $CuCr_{1-x}Mn_xO_2$ system if DE interaction occurs through Mn^{3+}–O–Cr^{3+}. Therefore, we investigated the magnetic property of the samples for $x < 0.30$.

3.3. Magnetic properties

Figure 5(*a*) shows the temperature dependence of the magnetization (M–T curve) of the $CuCr_{1-x}Mn_xO_2$($0 \leqslant x \leqslant 0.20$) samples, where a 1 T magnetic field was applied. The inset of figure 5(*a*) shows the region of the dotted line in figure 5(*a*) in order to clearly present the M–T curves at a low temperature. It can be clearly seen that all the samples are in the paramagnetic states in the temperature range 120–300 K. The magnetization of the samples increases with increasing Mn concentration. For $x = 0.00$, an anomaly appears at 25 K owing to an antiferromagnetic (AFM) transition. The Néel temperature (T_N) is almost consistent with the one previously reported [26]. For $x = 0.05$ and 0.10, the M–T curves exhibit similar shapes when the temperature is greater than 30 K. Abrupt increases in magnetization appear at about 95 K shown in the inset of figure 5(*a*). It implies a FM transition which should be due to the FM interaction through the Mn^{3+}–O–Cr^{3+} exchange for $x = 0.05$ and 0.10. The magnetization reaches a maximum at 18 K and then decreases for $x = 0.05$, which is attributable to the AFM transition, whereas the AFM transition does not appear in the whole temperature range for $x = 0.10$ and 0.20. But then a tiny anomaly in the M–T curves can be seen at about 30 K, which is due to the AFM interaction. For $x = 0.20$, the FM transition

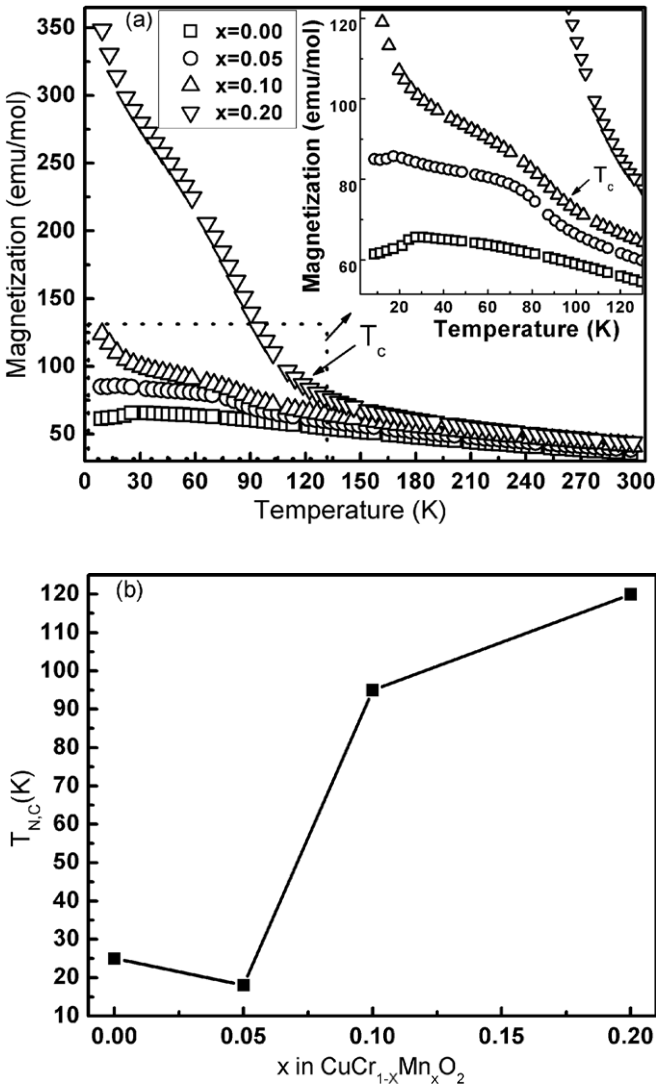

Figure 5. (*a*) Temperature dependent magnification (M–T) curves of $CuCr_{1-x}Mn_xO_2$ ($0 \leqslant x \leqslant 0.20$) semiconductors at a magnetic field of 1 T; the upper-right inset is the region of the dotted line. (*b*) The relationship between the critical temperature $T_{N,C}$ and the Mn concentration x.

temperature (Curie temperature T_c) is about 120 K. The FM interaction is clearly stronger than the AFM interaction as the Mn concentration increases. All these changes in the M–T curves indicate a competition between AFM and FM interactions for $0.05 \leqslant x \leqslant 0.20$, and also indicate that the DE interaction between the Mn^{3+} and Cr^{3+} ions is weaker in the $CuCr_{1-x}Mn_xO_2$ system. In figure 5(*b*) the critical temperature $T_{N,C}$ is shown as a function of the Mn concentration. The change in the critical temperature suggests that the FM interaction between the Mn^{3+} and Cr^{3+} ions increases with increasing Mn concentration. Plots of the inverse molar susceptibility $1/\chi$ as a function of the temperature for the $CuCr_{1-x}Mn_xO_2$ ($0 \leqslant x \leqslant 0.20$) samples are shown in figure 6. The plot of $1/\chi$ versus T shows an exactly linear relation at high temperature, which is well fitted by the Curie–Weiss equation, $\chi = C/(T + \Theta)$ [27]. It indicates that all the $CuCr_{1-x}Mn_xO_2$ ($0 \leqslant x \leqslant 0.20$) samples are paramagnetic states at high temperature, while the curves show some nonlinear behaviour

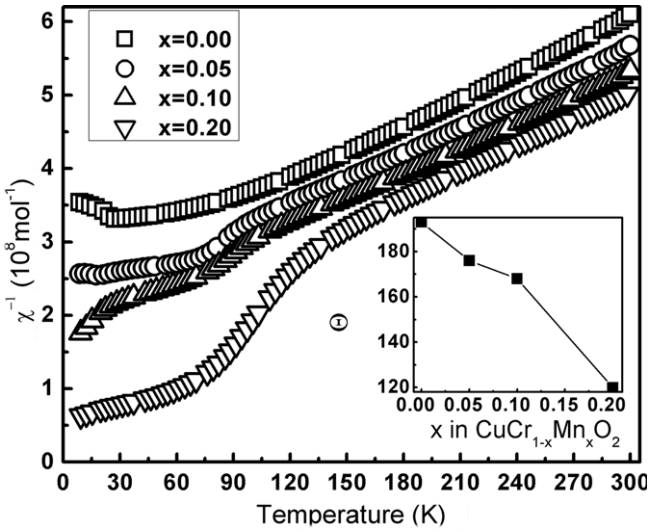

Figure 6. Temperature dependence of the inverse susceptibility of $CuCr_{1-x}Mn_xO_2$ as a function of the temperature; the inset shows the variation of the Curie–Weiss temperature Θ with the Mn concentration x.

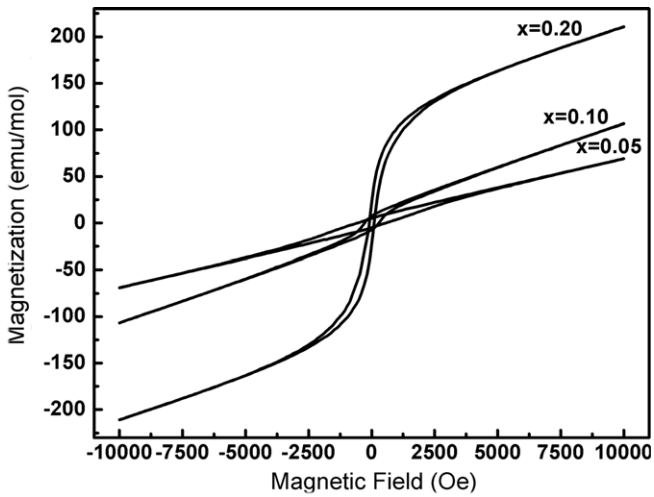

Figure 7. M–H relationship of $CuCr_{1-x}Mn_xO_2$ ($x = 0.05$, 0.10 and 0.20) at 50 K. Clear hysteresis loops are observed, confirming a FM order induced by Mn doping in $CuCrO_2$ semiconductors.

attributed to AFM or FM interaction at a low temperature. The relationship between x and the Curie–Weiss temperature (Θ) which can be obtained by the Curie–Weiss equation is shown in the inset of figure 6. The FM behaviour of the $CuCr_{1-x}Mn_xO_2$ ($0 \leqslant x \leqslant 0.20$) semiconductors was further investigated as a function of the applied magnetic field. The magnetic field dependence of magnetization (the M–H curve) of the $CuCr_{1-x}Mn_xO_2$ ($0 \leqslant x \leqslant 0.20$) semiconductors was measured at 50 K, as shown in figure 7, which reveals clear hysteresis loops indicating that the FM order exists in the materials at a low temperature. The Mn^{3+}–O–Cr^{3+} exchange interaction was extensively studied in the $LaMn_{1-x}Cr_xO_3$ system. Gundakaram *et al* [28] and Deisenhofer *et al* [29] proposed that the Mn^{3+}–O–Cr^{3+} exchange interaction is superexchange (SE). Zhang *et al* pointed out the possibility of Mn^{3+}–O–Cr^{3+} DE interactions in $LaMn_{1-x}Cr_xO_3$ in order to correlate their electronic transport data with the magnetic property in their samples [30]. Sun *et al* suggested that the DE of Mn^{3+}–O–Cr^{3+} would be weaker than that of Mn^{3+}–O–Mn^{4+}, which leads to the absence of a metallic state in the FM phase [23]. Morales *et al* studied the resistivity and susceptibility in the paramagnetic region and showed a clear signature of the DE interaction between the Mn^{3+} and Cr^{3+} ions [22]. And they testified to the DE mechanism in the $LaMn_{1-x}Cr_xO_3$ system by calculating the band model of $LaMn_{1-x}Cr_xO_3$. In this research the FM interaction was confirmed by the M–T curves of the $CuCr_{1-x}Mn_xO_2$ ($0 \leqslant x \leqslant 0.20$) samples. And the relationship between the resistivity and Mn concentration of $CuCr_{1-x}Mn_xO_2$ ($0 \leqslant x \leqslant 0.20$) samples can be well interpreted by the DE mechanism. The resistivity of the doped samples is larger than that of the pure $CuCrO_2$ semiconductor, which reveals that the DE interaction between the Mn^{3+} and Cr^{3+} ions is weaker in the $CuCr_{1-x}Mn_xO_2$ system. In addition, it is also possible that the FM order in the $CuCr_{1-x}Mn_xO_2$ semiconductors originates from some unknown phases in the $CuCr_{1-x}Mn_xO_2$ system.

4. Conclusion

In summary, we have prepared polycrystalline p-type $CuCr_{1-x}Mn_xO_2$ ($0 \leqslant x \leqslant 0.30$) semiconductors using the sol–gel method. No secondary phase was observed for $x \leqslant 0.20$ in our samples. The lattice parameters increase as the Mn concentration increases. The valence state of Mn ions is 3+ in the $CuCr_{1-x}Mn_xO_2$ semiconductors. The $CuCr_{0.80}Mn_{0.20}O_2$ semiconductor exhibits a clear FM transition which was ascribed to originating from the DE interaction between the Mn^{3+} and Cr^{3+} ions. The origin of the ferromagnetism in DMS is still under debate. The free-carrier mediated DE mechanism was supposed to be the origin of ferromagnetism in Co-doped ZnO [31], (Ga, Mn)N [32] and (Ga, Mn)As [33]. Our research supported the DE mechanism once again.

Acknowledgments

This project was financially supported by the Chinese National Natural Science Foundation (No 50672097) and by the Chinese Academy of Sciences under the Program for Recruiting Outstanding Overseas Chinese (Hundred Talents Program).

References

[1] Jung S W, An S-J, Yi G-C, Jung C U, Lee S-I and Sunglae C 2002 *Appl. Phys. Lett.* **80** 4561
[2] Munekata H, Ohno H, von Molnar S, Segmüller A, Chang L L and Esaki L 1989 *Phys. Rev. Lett.* **63** 1849
[3] Ohno H, Shen A, Matsukura F, Oiwa A, Endo A, Katsumoto S and Iye Y 1996 *Appl. Phys Lett.* **69** 363
[4] Dietl T, Ohno H, Matsukura F, Cibert J and Ferrand D 2000 *Science* **287** 1019
[5] Wakano T, Fujimura N, Morinaga Y, Abe N, Ashida A and Ito T 2001 *Physica* E **10** 260
[6] Ueda K, Tabata H and Kawaib T 2001 *Appl. Phys. Lett.* **79** 988
[7] Pearton S J, Heo W H, Ivill M, Norton D P and Steiner T 2004 *Semicond. Sci. Technol.* **19** R59

[8] Hoffman R L, Norris B J and Wager J F 2003 *Appl. Phys. Lett.* **82** 733
[9] Qiao Z, Latz R and Mergel D 2004 *Thin Solid Films* **466** 250
[10] Kawazoe H, Yasukawa M, Hyodo H, Kurita M, Yanagi H and Hosono H 1997 *Nature* **389** 939
[11] Nagarajan R, Draeseke A D, Sleight A W and Tate J 2001 *J. Appl. Phys.* **89** 8022
[12] Zhang H Y, Li P G, Chen C P, Tu Q Y and Tang W H 2005 *J. Alloys Compounds* **396** 40
[13] Kizaki H, Sato K, Yanase A and Katayama-Yoshida H 2005 *Japan. J. Appl. Phys.* **44** L1187
[14] Li D, Fang X D, Deng Z H, Zhou S, Tao R H, Dong W W, Wang T, Zhao Y P, Meng G and Zhu X B 2007 *J. Phys. D: Appl. Phys.* **40** 4910
[15] Kamiharaa Y, Matoba M, Kyomen T and Itoh M 2002 *J. Appl. Phys.* **91** 8864
[16] Weaver J F, Hagelin H A E, Hoflund G B and Salaita G N 2006 *Appl. Surf. Sci.* **252** 7895
[17] Lu W J, Sun Y P, Ang R, Zhu X B and Song W H 2007 *Phys. Rev.* B **75** 014414
[18] Shi L, Li G, Feng S J and Li X G 2003 *Phys. Status Solidi* a **198** 137
[19] Bertoni M I, Mason T O, Medvedeva J E, Wang Y Q, Freeman A J and Poeppelmeier K R 2007 *J. Appl. Phys.* **102** 113704
[20] Sun Y, Wei T, Xu X J and Zhang Y H 2001 *Appl. Phys. Lett.* **78** 643
[21] Zener 1951 *Phys. Rev.* **82** 403
[22] Morales L, Allub R, Alascio B, Butera A and Caneiro A 2005 *Phys. Rev.* B **72** 132413
[23] Sun Y, Tong W, Xu X and Zhang Y H 2001 *Phys. Rev.* B **63** 174438
[24] Nakazono S, Ono K and Oshima M 2001 *J. Magn. Magn. Mater.* **226–230** 866
[25] Morales L and Caneiro A 2003 *J. Solid State Chem.* **170** 404
[26] Kadoeaki H, Kikuchi H, and Ajiro Y 1990 *J. Phys.: Condens. Matter* **2** 4485
[27] Okuda T, Jufuku N, Hidaka S and Terada N 2005 *Phys. Rev.* B. **72** 144403
[28] Gundakaram R, Arulraj A, Vanitha P V, Rao C N R, Gayathri N, Raychaudhuri A K and Cheetham A 1996 *J. Solid State Chem.* **127** 354
[29] Deisenhofer J, Paraskevopoulos M, Krug von Nidda H-A and Loidl A 2000 *Phys. Rev.* B **66** 054414
[30] Zhang L W, Feng G, Liang H, Cao B S, Zhu M H and Zhao Y G 2000 *J. Magn. Magn. Mater.* **219** 236
[31] Sato K and Katayama-Yoshida H 2001 *Physica* B **308** 904
[32] Sato K, Schweika W, Dederichs P H and Katayama-Yoshida H 2004 *Phys. Rev.* B **70** 201202
[33] Wierzbowska M, Sánchez-Portal D and Sanvito S 2004 *Phys. Rev.* B **70** 235209